Development of a Soft Actuator from Fast Swelling Macroporous PNIPAM Gels for Smart Braille Device Applications in Haptic Technology

Refik Baris Yilmaz, Yosr Chaabane, Vincent Mansard

Development of a soft actuator from fast swelling macro-porous PNIPAM gels for smart Braille device applications in haptic technology

Refik Baris Yilmaz, Yosr Chaabane, and Vincent Mansard*

CNRS, LAAS-CNRS, 7, avenue du Colonel Roche, BP 54200 31031, Toulouse Cedex 4, FRANCE

E-mail: vincent.mansard@laas.fr

Abstract

Development of a cost-efficient Braille device is a crucial challenge in the haptic technology to improve integration of visually-impaired people. Exclusion of any group threatens the proper functioning of the society. Commercially available Braille devices still utilize piezo-electric actuators which are expensive and bulky. The challenge of more adapted Braille device lies in the integration of a high number of actuators—of a millimetric scale—in order to move independently a matrix of pins acting as tactile cues. Unfortunately no actuation strategy happens to be adapted to tackle this challenge. In this study, we develop a soft actuator based on a thermosensitive poly(n-isopropylacrylamide) (PNIPAM) gel. We introduce macroporosity to the gel (pores of 10 to $100\,\mu m$). It overcome the diffusion—which is the limiting kinetic factor—and accelerate the gel response time from hours for bulk gel to seconds for macroporous gel. We study the properties of porous gels with various porosity. We also compare mechanically reinforced nanocomposite gel (made of PNIPAM and Laponite clay) to "classic" gel. As a result, we develop a fast actuating gel with high cyclic performance. We then develop a single pin Braille setup, where actuation is controlled thanks to a swift temperature control of a macroporous gel cylinder. This new strategy offers a very promising actuation technology. It offers a simple and cost-efficient alternative to the current Braille devices.

Keywords

Haptic, Braille, Hydrogel, Poroelasticity, PNIPAM, Soft Actuator, Thermo-Sensitive

1 Introduction

Adaptation of the numerical technologies to people with visual impairments is a major social challenge. The current human-computer interaction—based on screen—is highly unadapted to them. The rapid spread of touchscreens, which do not offer any tactile feedback amplify this exclusion. To tackle this challenge, there is a crucial need for the expansion of deformable displays, where tactile cues–such as pins–can appear and disappear.[1–4] Beyond the context of visual impairment, sighted users involved in a visual attention task (e.g. driving or piloting) could also use such deformable screens.

In the 90s, the first Braille displays–based on piezo-electric actuators–appeared.[1,5–8] They allow displaying dynamically 20 to 80 Braille characters. Nevertheless, the small deformation ratio of piezo-electric material imposes to use large quantity of material. Therefore, Braille displays remain expensive and bulky. The integration of blind people requires going beyond the display of few Braille characters. It would require the development of smart Braille tablet with a high density of pins to be able to display not only text but also complex graphical information. To be sensed with a finger, a pin needs to have at least 1.4 mm of diameter, and 0.1 mm of height while being able to support a force of 50mN (5g).[6]

The key challenge of such tactile surface relies on the complexity to actuate a high number of pins independently.[1,9] It would require low cost millimetric actuating systems. Several strategies have been explored based not only on piezo-electric systems but also on pneumatic actuation,[10,11] magnetic actuation[12–14] or others.[15–19] Today none of these strategies have reached the commercialized

status.

In this article, we explore a new actuation strategy using mechanically active gel which are called smart gels.[20–22] We particularly focused on thermosensitive gels based on poly(n-isopropyl acrylamide) (PNIPAM).[23,24] PNIPAM gel shows a volume phase transition with temperature. For temperatures above 34°C, PNIPAM gel shrinks reversibly with a very large swelling ratio (i.e. volume ratio between a swollen and shrunk gel sample), which can reach 1000 %.[25,26]

This large volume change is due to a modification of the solubility of the PNIPAM, which induces transfer of water in or out of the polymer matrix.[23,27,28] The NIPAM monomer contains a hydrophilic amide and a hydrophobic propyl moiety. The prevailing characteristic of each moiety changes with the temperature. This results in a conformational change of molecules from random coil (hydrophilic) at low temperature to globule (hydrophobic) at high temperature.

PNIPAM gels are commonly used for drug delivery,[29,30] dosimeter[31,32] and biosensing[33] applications. Few studies have demonstrated that it can also be used for soft actuation purposes.[34,35] PNIPAM gel shows several key characteristics suitable for development of a smart Braille tablet. Thanks to the very large swelling ratio, only a small quantity of active material is required to produce large enough displacement (actuation). Furthermore, controlling the actuation only requires to locally control the temperature. It can also be implemented relatively easily with small heating resistances. Furthermore, the low temperature transition (below 40°C) is user-friendly and safe with no risk to burn the user's finger.

Hydrogel face two major limitation for actuation: a high fragility of the hydrogel and very slow response to stimuli. In this article, we combine two recent developments to overcome these limitation. The first development is the synthesis of hydrogel with improved mechanical robustness[36–40] — often called *tough gel*. The second one is the synthesis of fast reacting gel with macroporous structure.[41] These two scientific leaps — which make smart gel adapted to soft actuation — are discussed underneath.

The last decade have known the synthesis of new type of hydrogel with very high robustness.[36–40] These *though gels* eventually show maximum strain and fracture energy comparable to elastomer. They are based on innovative synthesis approaches and new types of polymer networks which include double polymer networks[36–38] (which is the most studied strategy) or nanocomposite (NC) hydrogels.[39,40,42–44]

Nanocomposite (NC) gels are made of hard nanoparticles incorporated into the polymer matrix to enhance the mechanical properties.[40,45–47] PNIPAM-Clay NC gel is a promising candidate for actuation. It is particularly simple to synthesize based on a one-pot process. Furthermore it shows very good mechanical properties, which can be tuned by adjusting the clay concentration. The clay is used as physical crosslinking agent.[48,49] Indeed the clay is made of electrically charged disk-shaped nanoparticles, which act as reticulation nodes.

The second recent improvement is the acceleration of the gel actuation of smart gel. The swelling kinetics of smart gels is controlled by the diffusion of water through the polymer matrix.[50,51] Bulk hydrogels behave as a poro-elastic media with pore size of about 10 to 100 nm in diameter. Because of this small pore size, bulk gels are very slow to swell. Gel samples of 1.0 cm size take from hours to days to swell or shrink. Thus, fast actuation is only obtained for thin layer of bulk gels below 100 μm of thickness in which diffusion rate limitation is eliminated.[52]

Synthesizing gels with larger pores facilitates the solvent transfer and accelerates the swelling speed.[41,53] Macroporous gels (MP gels) with pore sizes of about 10 to 100 μm in diameter show fast enough reaction for soft actuation. Thus, many methods have been developed for induction of macro porosity on hydrogels such as incorporation of sacrificial templates,[41,53,54] sacrificial additives (e.g. poly(ethylene glycol))[55] or solvent freezing.[45,52,56,57]

Freezing the solvent contained into the gel offer a quick way to generate pores. For instance Gil et al.[58] generated macropores with a diameters of 380 μm on PNIPAM gel by freeze drying. They were able to decrease the actuation time of macroporous PNIPAM/Silk hybrid hydrogel from 24 hours to 1 minute. Nevertheless solvent freezing offer poor control on the pores structures, which highly depends on the freezing kinetics and therefore on the gel sample shape. At the opposite, porosity based on the sacrificial template offer better control. For instance, Zhao et al.[54] developed macroporous PNIPAM gels with tunable pores size between 20 to 70 μm using sacrificial dimethyl benzyl

ammonium bromide (DDBAB) particles, reducing the actuation time down to 1 minute. In a similar strategy, Warren et al.[41] synthesized macroporous PNIPAM-alginate hydrogel using sacrificial shellac fibers. The specific fiber shape of the sacrificial template is particularly adapted. It ensure the pores to be interconnected for good solvent transfer and fast actuation speed.

In this study, we investigate a new type of thermosensitive PNIPAM gel for the actuation in a Braille tablet. This material combine high robustness, large swelling amplitude and fast actuation speed. To achieve this goal, we synthesize *tough* clay nanocomposite hydrogel with a macroporous structure obtained from a sacrificial template. We compare the properties of mechanically enhanced nanocomposite gel (NC gel) to "classical" organically reticulated gel (OR gel), which is produced by the radical polymerization of NIPAM in presence of a divalent crosslinker molecule.

In a first part, we characterize the macroporous gels (MP gels). We particularly focus on the shrinking-re-swelling kinetics and on the mechanical response to compression of the different gel sample. We demonstrated the specificity the two polymer network (NC vs OR gels) and compare the influence of two different porous structure. We demonstrate the limit of NC gel. But we shows that OR MP gel present very adapted properties. In a second step, we demonstrate that PNIPAM MP gel can efficiently be used for actuation. We build a prototype of a cost-efficient Braille system. A cylinder of MP gel is used to actuate vertically a pin of few millimeters. The actuation is controlled through the control of temperature with a heat resistance and Peltier plate for respectively heating and cooling. Our prototype is limited to one pin. But our heating/cooling strategy could be easily implemented to actuate several pins.

2 Results

2.1 Characterization of MP Gel

We produced macroporous gel (MP gel) samples by polymerizing a monomer NIPAM solution around a solid template. We then remove the template by selective dissolution. We consider 2 types of templates, which gave two different porosities (i.e. void fraction) [Fig.1a-b].

We produced gel with high porosity (HP gel) by using a template made of poly(methyl methacry-late) (PMMA) microspheres (diameter 100 µm) [Fig.2c]. Particles are first sintered at 185°C for 8h. Sintering ensure solid contact between particles in order to obtain interconnected pores. Packing of spherical particles are naturally dense and the density of template is measured to be about 60% in agreement with previous study.[53]

To obtain gel with low porosity (LP gel), we use a second type of template made of shellac fibers. We produce microfibers (diameter 12 µm) by melt spinning[41] [Fig.2a]. We then wash the fibers in pure water and pack them into a Petri dish to form a fiber mat. Shellac is naturally insoluble in water but easily dissolved in NaOH solution. The low melting temperature of shellac (75°C) makes it well adapted for melt spinning. The fiber structure enables to tune the template density. The resulting pores will be interconnected independently of this density. We pack the fibers to obtain a mat density of about 15%.

The properties of the gel matrix are also crucial to control the mechanical properties of the MP gel. Thus, we consider two types of gels [Fig. 1c-d]: "classical" organically reticulated (OR) gel and nanocomposite (NC) gel where PNIPAM chains are cross-linked through clay nanoparticles (Laponite RDS).

To produce OR gels, we prepare a solution of NIPAM with acrylamide as cross-linker and Irgacure 651 as UV-sensitive initiator. Solutions are poured on the solid template (PMMA template or shellac fiber) and polymerization is performed under UV light.

We produce NC gel by first dissolving NIPAM and Laponite RDS under high stirring. We purge the solution with nitrogen to remove dissolved oxygen. We then initiate the polymerization by adding APS and TEMED. The concentration of APS and TEMED is carefully chosen to obtain a polymerization within 24h. The solution is then poured onto the shellac fiber mat (NC gel is not compatible with PMMA templating as we will discuss later). Precise control of the experimental condition is important. Small change of concentration or temperature would lead to a too fast gelification or to no gelification at all.

Finally, we obtain MP gel by selectively dissolving the template. For HP-gel, we remove the PMMA scaffold by 4 successive 24h bath in ethyl acetate followed by rinsing the gel in ethanol before swelling back the gel in water [Fig.1a]. It is not possible to produce NC gel with a PMMA template as
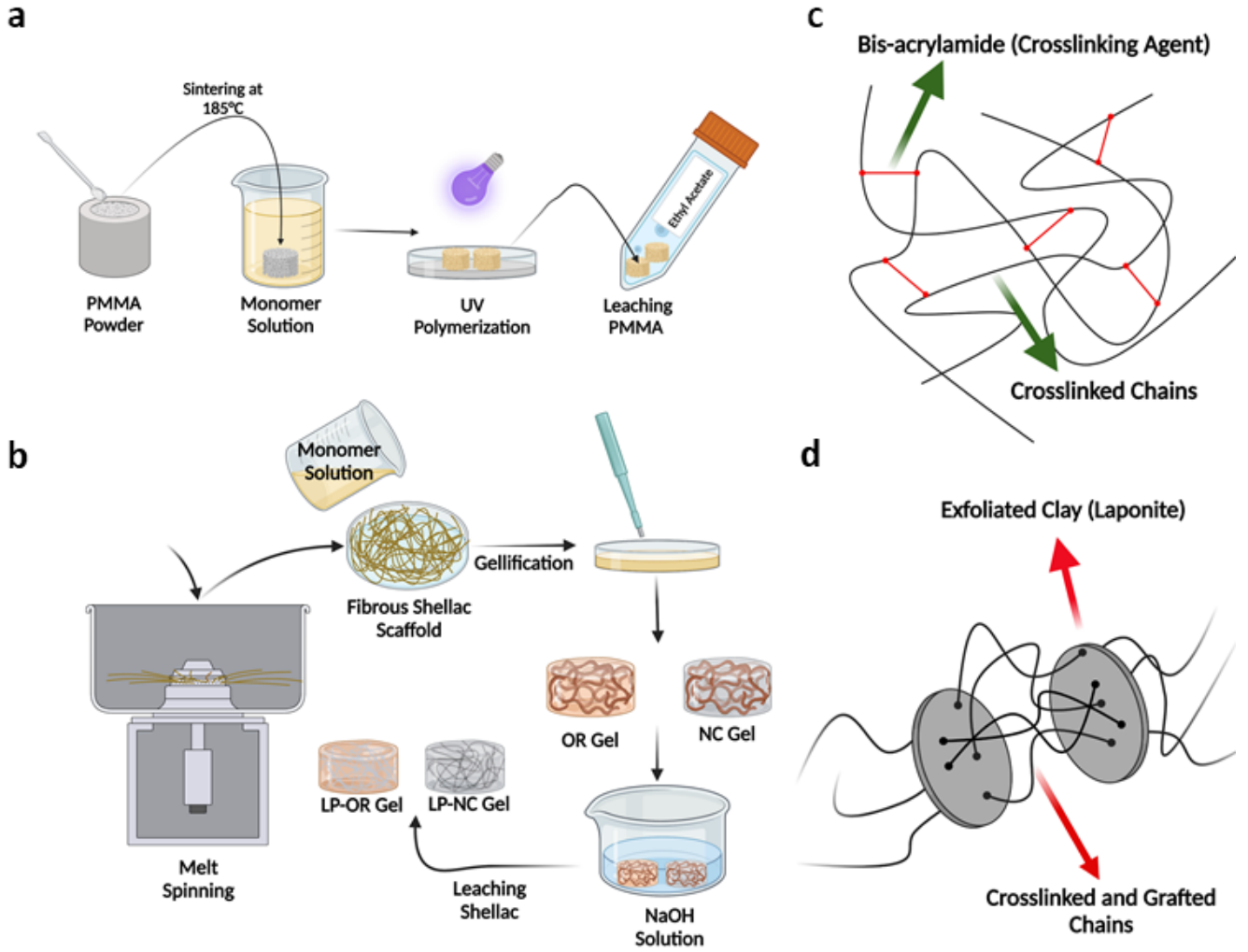
3

Figure 1: Schematic representation of macroporous gel (MP gel) synthesis for (a) high porosity (HP) gel based on PMMA spherical particles and (b) low porosity (LP) gel based on shellac fibers. Schematics of intermolecular crosslinks in (c) organic reticulated (OR) gel and (d) nanocomposite (NC) gel.

NC gel gets dissolved in ethyl acetate. Therefore, we only consider HP-OR gels.

For LP gels, with first cut samples with the required dimension from the gel + fiber mat. We then dissolve the shellac fibers in 3 successive baths of NaOH and rinse samples in pure water [Fig.1b]. This process is gentler with hydrogel as it does not require to change solvent. Both LP-OR gels and LP-NC gels have been produced.

We observe a good agreement between the shape of the initial scaffold observed by SEM [Fig.2a&c] and the structures of the resulting MP gels observed by microscopy [Fig.2b&d]. Our synthesis process does not creates voids. Therefore, the gel porosity (i.e. void fraction) is likely to be equal to the scaffold density and can be estimated to be $\rho = 60\%$ for HP gel and $\rho = 15\%$ for LP gel.

We can also estimate the pore sizes from the SEM images of the scaffold. The average diameters of spherical PMMA particles and shellac fibers are determined to be 75 ± 30 µm and 12 ± 5 µm, respectively. The average diameter of the fibers and spherical particles are determined from the SEM images. It was unfortunately not possible to obtain fibers with similar sizes as PMMA particles.

In order to determine the shrinking rate of the MP gel, we dip a cylindrical sample of gel (d×h=7 × 10 mm) into a hot water bath (60°C) [Fig.3a]. We observe a very fast color change—within 1s—from transparent to white. It is followed by the gel shrinking [Fig.3d]. The color change is due to the PNIPAM molecular transition from random coil to globular (which happens around 34°C). It demonstrates a very fast tempera-
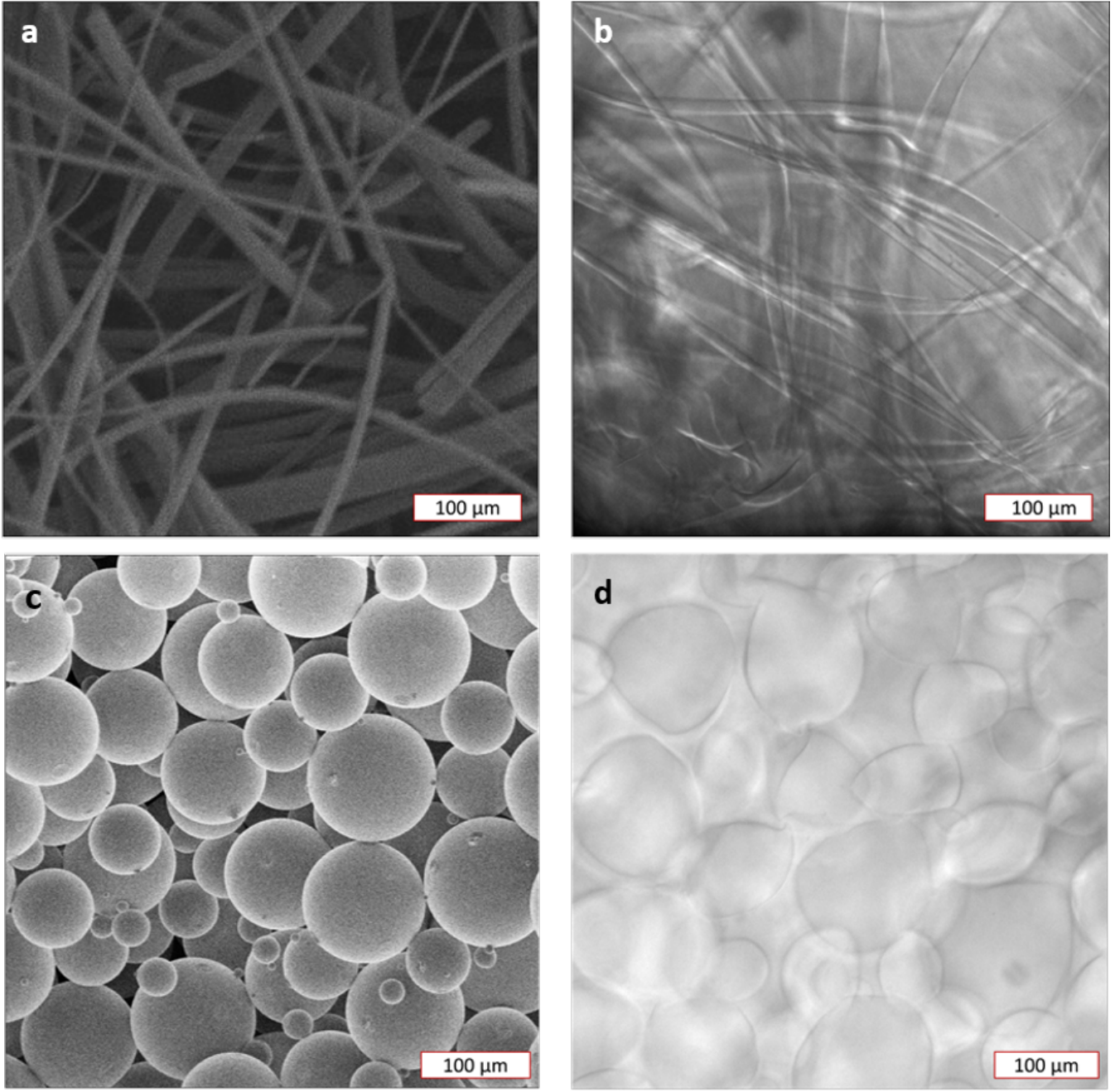
4

Figure 2: (a&c) SEM images of the sacrifical template: (a) melt spun shellac fibers and (c) PMMA microspheres. (b&d) image of the MP gel using DIC microscopy to observe the macroporosity: (b) LP-OR gel and (d) HP-NC gel. SEM images and DIC microscopy images are at the same scale to emphasize the similarity between the initial sacrificial scaffold and the final porosity. No SEM images of the porous gels are shown here as drying the gel dramatically affect the gel structure.

ture increase. Thus, the delay for shrinking should only be due to the time required for solvent transfer.

We quantify the dynamics of volume variation using visualization with a camera. We measured the observed surface area of the gel at each time with a simple image recognition algorithm on ImageJ. We deduce the evolution of volume as the size variation is isotropic. This method offers a good temporal resolution. In parallel, similar gel samples are also dipped and kept in hot water to be periodically weighed. This second experiment is implemented to observe the long-term changes (hours to days) in PNIPAM gel volumes upon heating.

MP gels show a much faster shrinking dynamics than bulk gels as expected [Fig.3b]. 20s after the
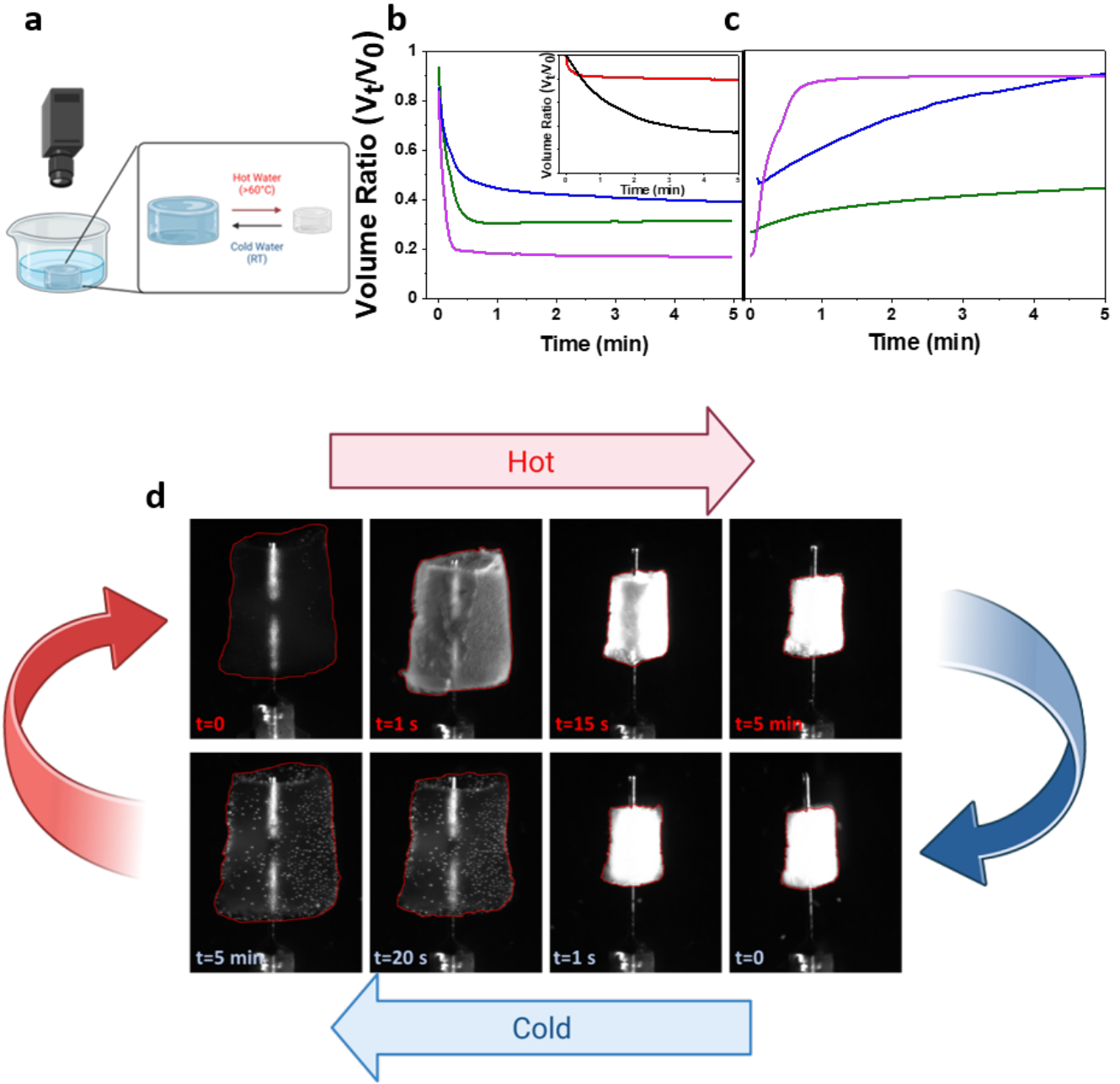
Figure 3: (a) Schematic of the real time imaging setup for the shrinking re-swelling tests. (b-c) Evolution of the volume ratio V/V_0 (where V_0 is the initial gel volume at room temperature before shrinking) as function of time when the gel is successively dipped (b) in hot water and then (c) in cold water for (Blue) LP-OR, (Green) LP-NC, (Pink) HP-OR gel. (inset) Dynamic of shrinking for bulk gel: (Black) NC gel, (Red) OR gel. (d) Typical images of HP-OR gel during shrinking re-swelling process.

temperature increase, bulk OR gel and bulk NC gel only shrink to 90% and 80% of their initial volume, respectively. Whereas in the same time scale, LP-OR and LP-NC gels shrink to 50% and 40% of their initial volume, respectively. Furthermore, HP-OR gels shrink to 20% in the first 20 s thanks to the higher porosity and larger pore sizes.

LP-NC gel shrinks faster than LP-OR gel. It has been previously observed for bulk gels.[48] This acceleration is due to the presence of clay nanoparticles. They help to obtain larger nanopores. They also avoid the formation of a hydrophobic skin layer which prevent the water to be transported out of the gel.

After 30 s, the volume ratio of MP gels reaches a plateau phase. The volume reached at the plateau

6

depends on the gel porosity. It is equal to 20%, 30% and 50% of the initial volume for respectively HP-OR, LP-NC and LP-OR gels. This plateau is actually a pseudo-equilibrium stage. MP gel keeps shrinking very slowly (less than 1% of volume change over 15 min). All samples reach about 10% of the initial volume after 24h in hot water.

During the gel shrinking, the size of the pores decreases and eventually closes up. The pore closure would explain this pseudo-equilibrium state. Introduction of larger pores–larger nanopores for LP-NC gel or larger macropores for HP-OR gel–helps to drain the water out of the gel. But it does not prevent the pore closure and the apparition of pseudo-equilibrium where the gel is not fully shrunk. For actuation, we cannot use the full amplitude of volume variation—i.e. a volume changing by a factor 10 between swollen and shrunk state. We can only use a smaller fraction of the amplitude—volume change by a factor 5, 3 and 2.5 respectively for HP-OR, LP-NC and LP-OR gel.

We then study the gel re-swelling dynamic. To do so, we take the hot gel samples (which have been at 60°C for 5 min) and transfer them quickly to a water bath at room temperature (about 20°C). Once again, we observe a very fast color change (from white to transparent) followed by the gel swelling.

The re-swelling dynamic does not show the same behavior as for the shrinking. We need to distinguish OR and NC gels at this point [Fig.3c]. For OR gels we observe that introduction of macroporosity highly accelerates the swelling as expected. While it took a day for the bulk OR gel to regain 88% of its initial volume upon re-swelling, LP-OR and HP-OR gels needed only 4.5 and 1 minutes, respectively.

Nevertheless, we observe that re-swelling is significantly slower than shrinking. Such asymmetry with a slow re-swelling has been also observed for bulk PNIPAM gel.[45,48,55,58,59] However, no extensive insight on this phenomenon is available. The slow re-swelling is thought to be due to the hysteresis upon fully closed (collapsed) pores resisting the inwards solvent diffusion.

The difference of dynamic cannot be due to different heat transfer kinetic when we heat up and when cool down the gel sample. The temperature change is produced by dipping the gel in a very large excess of water. So heating and cooling happens at the same rate. Furthermore we observe a very fast color change of ~ 1 s which indicate a very fast transition of molecular conformation between globular and random coil. To emphasize that heat transfer has no impact on the shrinking/swelling dynamic, we reproduce the experiments using a cold water bath at 3 different temperatures: 20 °C, 7 °C and 0 °C. We observe no significant difference of dynamic between the 3 different temperatures.

To better understand, the kinetic limitation in OR gel, we produced gel with high porosity but smaller pore sizes of 60 μm. This gel is called HP $_{60\,\mu m}$-OR gel. It is produced with the same process than regular HP-OR gel but using smaller PMMA particles (diameter 60 $\pm$ 20 μm). We observe a slightly faster dynamic of shrinking and swelling than for regular HP-OR gel [Table 1]. It proves that convection through the macropores is not a limiting process as convection would be slow down for smaller pores. For HP-OR gel, the limiting kinetic factor remain the solvent diffusion through the gel walls to the macropores.

Re-swelling of the LP-NC gel is much slower than LP-OR gel. During the initial 5 min, LP-NC gel re-swells to only 45 % of its initial volume whereas LP-OR gel reaches 90% . Actually LP-NC re-swells even slower than bulk OR despite its macro porosity. And we observe a very similar swelling dynamics for both bulk and macroporous NC gel. These results suggests that the swelling kinetic of NC gel is not limited by the solvent transfer.

The very different timescale for swelling demonstrates that different limiting factor are involved

Table 1: Shrinking/re-swelling and modulus data of porous PNIPAM gel samples. t_{shrink} represents the time required for the gel to reach 50% of its initial volume whereas t_{swell} is the time required to reach 80% of the initial volume.

	Porosity	Pseudo-Equilibrium Volume (%)	t_{shrink}	t_{swell}	E (KPa)	Used in the Braille Device?
NC	LP	30	10 s	>6h	4	-
OR	LP	50	21 s	3 min	18	-
	HP	20	4 s	18 s	3	Yes
	HP$_{60\mu m}$	15	2 s	12 s	1	-

for OR and NC gel. The slow dynamic of NC gel is probably due to reorganization of the Laponite nanoparticles interacting at microscopic level. Indeed, Laponite is made of disc-shape nanoparticles carrying both positive and negative surface charges. They create electrostatic bonds between them to form house-of-cards like structure.[44] At high temperature, the gel shrinks and distance between nanoparticles decreases. Interaction between particles increases, which likely induce reorganization of the clay structure and formation of the new bonds. When we cool down the gel, this new clay network would prevent the gel to swell back. And the swelling kinetic is now controlled by the time required to disrupt the bonds between clay particles.

For actuation, it appears that the swelling kinetic of PNIPAM gel is the limiting aspect. Whereas the discussion in the literature is often limited to the shrinking kinetic. For NC gel, the introduction of macro porosity does not accelerate the swelling. Thus, NC gel cannot be adapted for actuation. On the contrary, MP gels based on OR gel show very interesting kinetic. Especially, HP-OR gel shows a swelling and shrinking within less than 30s—thanks to the very large porosity levels.

The fast MP gel response enables to easily obtain the volume variation as function of the temperature [Fig.4a]. MP gel samples are dipped in water bath at room temperature and heated on a hot plate. The volume change is recorded by imaging while measuring the temperature rise. The heating rate (1°C/min) is chosen slow enough to always be in the pseudo equilibrium stage.

We observe a sharp volume transition at about 34°C for the OR gels and 40°C for NC gel. The volume reached at high temperature depends on the gel type and on the porosity. It complies with the volume reached at the plateau during the previous experiment.

We now turn to the mechanical properties of MP gels. All gel samples have been characterized under compression–which corresponds to the deformation applied to the sample in the Braille setup. The samples show an elastic linear response at deformation $\epsilon < 20\%$ from which we extract the young modulus E [Fig.4b-c]. Bulk OR gel show a higher modulus than bulk NC gels. Actually, the modulus of our NC gels is lower than reported in literature.[44] Indeed, in our experiment the gel samples are kept in the water–and happens to swell–before measurement while in other articles, the modulus is measured right after synthesis.

Addition of macroporosity decreases the young modulus of the material. This decrease is dependent on the porosity. To characterize it, one calculate typically the modulus ratio between bulk material and porous material E_{bulk}/E_{porous}. If the modulus of the bulk material is the same as the modulus of the wall of the porous material, then the ratio depends only on the porosity ρ and is equal to:

$$\frac{E_{bulk}}{E_{porous}} = \frac{1}{(1-\rho)^2} \qquad (1)$$

For both LP-OR and LP-NC gels we found $E_{bulk}/E_{LP} = 1.3 - 1.5$ which is compatible with a porosity of $\rho = 15\%$.

For HP-OR gel, the porosity has stronger impact of the elastic modulus. We observe a modulus ratio $E_{bulk}/E_{HP} = 10$. This ratio is significantly larger than what we expected. It is not in agreement with Eq.1 and the estimated porosity $\rho = 60\%$. This discrepancy is amplified for $HP_{60\,\mu m}$-OR gel with a smaller pores size [Table 1]. This MP gel has the same porosity than regular HP-OR gel but shows a much lower modulus with $E_{bulk}/E_{HP60\,\mu m} = 28$. Furthermore, previous work studied MP gel made of polyacrylic acid (pAA) produced with the same protocol—and therefore presumably with the same porous structure—is studied.[53] pAA MP gels showed a modulus ratio $E_{bulk}/E_{porous} = 6$, which is in agreement with Eq.1.

This important gel weakening—characterized by a modulus ratio larger than expected— probably happens during the selective dissolution of the solid template. The dissolution requires the gel to be washed in ethyl acetate. It generates a change of solvent, which drives the gel to fully shrink. It creates important mechanical stress on the sample, which can explain the observed weakening once the gel is swollen back in water. We believe, that a process with no change of solvent would lead to MP gels able to sustain larger forces (about twice larger).

Introduction of porosity also improve the deformability and robustness of the gel. Bulk OR gel breaks from the compressive strain above 50%. LP-OR gel shows an improved maximum strain of 70%. HP-OR gel will fully recover its original shape even when compressed at the very high strain of 90% [Fig 4.d]. We tested all the MP gels under cyclic compression tests [Fig 4.e-g]. Even after 100
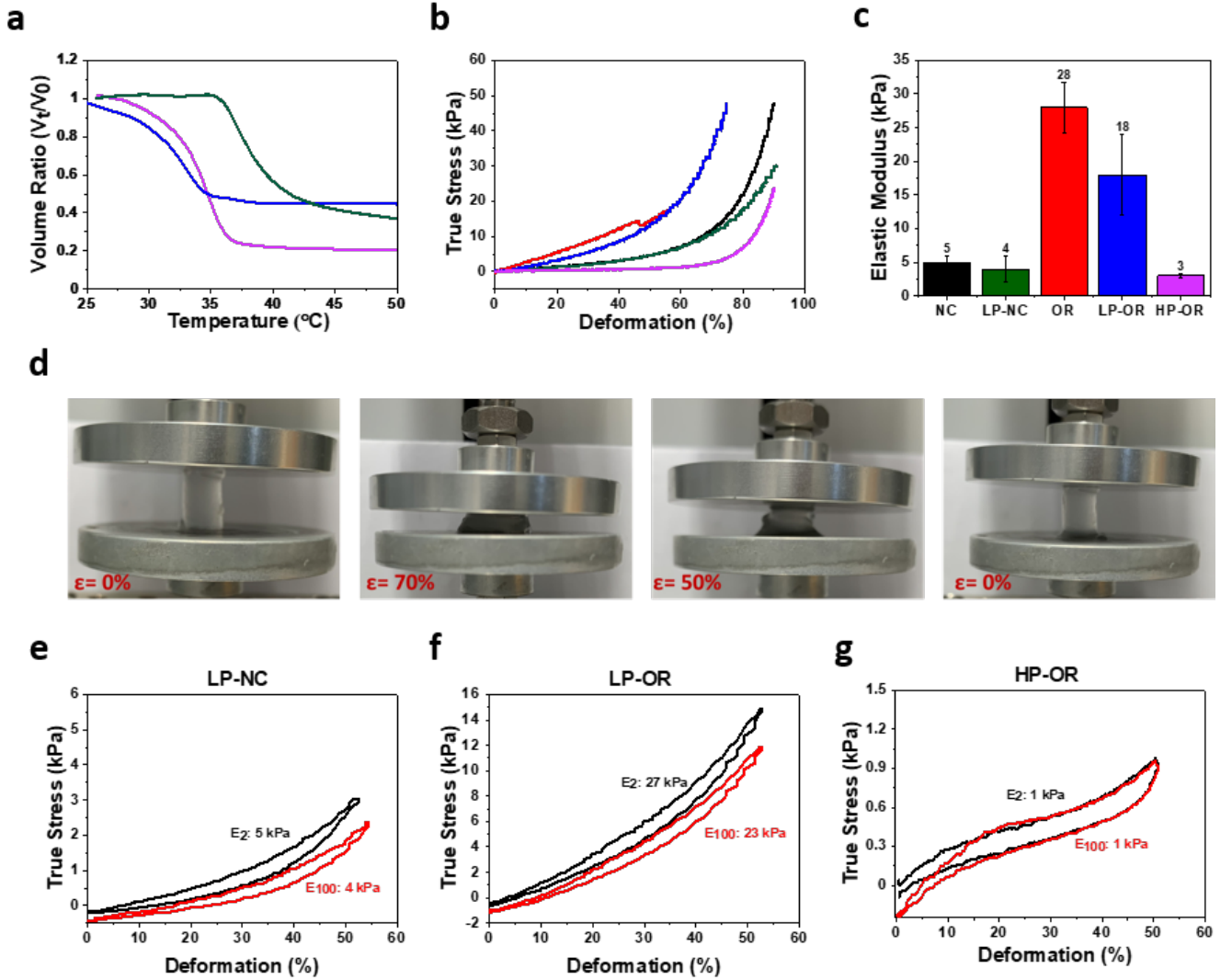
Figure 4: (a) Evolution of the volume ratios V/V_0 (where V_0 is the initial gel volume) as function of temperature when we slowly raise the temperature of the surrounding water bath (at $1\,°C/min$) for (Green) LP-NC, (Blue) LP-OR and (Purple) HP-OR gel. (b) True stress-strain curves of (Red) bulk OR, (Black) bulk NC, (Green) LP-NC, (Blue) LP-OR and (Pink) HP-OR gel. (c) Elastic Modulus values of the gel samples (same color coding). (d) Compression stages of HP-OR gel. (e-g) True stress versus strain graphs of gel samples under cycling deformation: (Black) first cycle and (Red) 100th cycle.

cycles, we observe only very small modification of the mechanical properties and their moduli are decreased by less than 15 %. In order to observe the tensile properties if the HP-OR gel, a tensile test is also conducted and the results such as tensile strength is presented in the supporting information [Fig.S3].

2.2 Fabrication of a Single Pin Braille Setup

To demonstrate the capacity of our new actuation strategy, we build a single pin Braille setup [Fig.5a-b]. It consists of 3D printed containment unit for the gel and water and a small pin which can move vertically through a hole in the center. A Peltier device (placed underneath the gel) and a nichrome electrical wire (wrapped around the gel) enable to respectively cool down and heat up the system. A thin stainless-steel sheet is folded into a cylinder and is placed between the gel cylinder and the nichrome wire. It improves temperature homogeneity. It also reduces the friction to facilitate displacement the plastic pin.

The nichrome wire has a high electrical resistance. It enables to heat the system by joule effect. The heating power of the nichrome wire is controlled between 0 and 7.75 W using pulse width
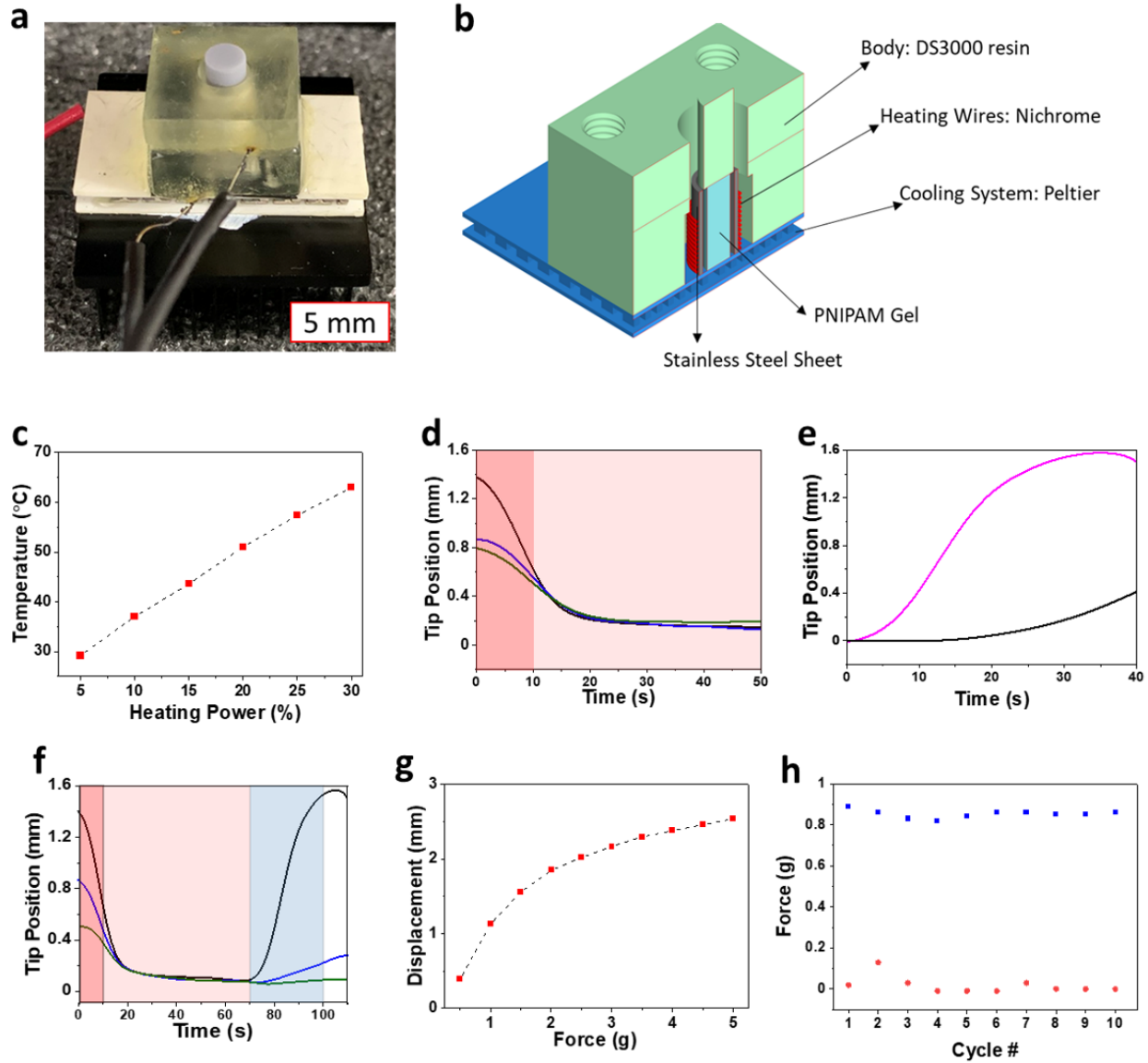
9

Figure 5: (a-b) Image and 3D representation of the single pin Braille setup. (c) Equilibrium temperature of the gel containment unit as function of the heating powers. (d) Evolution of the pin tip position as function of time during forced heating under (Black) no force or constant (Blue) 2.5g and (Green) 5.0g forces applied. The heating procedures is as described: (dark red) 100% power for 10 s and the (light red) 12% power. (e) Evolution of the pin position under (Black) natural cooling and (Blue) forced cooling. (f) Pin tip position during forced heating- forced cooling cycle under (Black) no force or constant (Blue) 2.5g and (Green) 5.0g forces applied. Heating procedure is as described previously. Forced cooling phase happens after 70 s and is shown in blue color. (g) Pin tip displacement versus applied force.(h) Minimum (red circle) and maximum (blue square) forces exerted by the Braille tip over ten heating-cooling cycles.

modulation (PWM) thanks to an Arduino microcontroller.

We first investigate the capabilities of our system to tune the temperature. A thermocouple is positioned in place of the gel cylinder inside the containment unit which is filled only with water. We heat the system at constant power and observe a quick increase of the temperature which reach an equilibrium temperature after ~2 min. Both the equilibrium temperature and the heating speed increase with the heating power. The equilibrium is nearly linear with the heating power [Fig.5c]. It reaches the transition temperature of 42°C for a heating power of only 12% and can go up to 65°C with 30% power. Higher power levels enable to obtain much faster heating and higher tempera-

tures. But they induce fast water evaporation. It is important to emphasize here that our PNIPAM hydrogel is always saturated and in contact with water. We do not operate the gel in dry or semi-dry state in any process.

Upon measurement of the dynamic temperature during heating, we constructed the optimum heating program. We quickly increase the system temperature up to 40°C by heating at 100% for 10s. We then maintain the temperature above 34°C by heating at 12%. This program ensures a very swift control over the temperature. We visually observed the gel during this heating procedure. We observed a quick color change (transparent to opaque white) of the entire gel cylinder—within less than a second—indicating a quick phase transition.

When we heat the system, we observe a rapid descent of the tip which start with few second delay. This delay corresponds to the time required to go above 34°C. We observe a descend of the pin of 1.2 mm within less than 30s [Fig.5]. After the 30s we observe that the pin keeps going down slowly (0.2 mm over 120s). This slow descent does not correspond to the slow gel shrinking observed in the pseudo equilibrium as the amplitude of the descent is too large. It is due to slow increase of the overall temperature of the system.

When we turn off the heating, the system cools down naturally. The cooling is slow and we observe that the tip ascends back to its initial position in 10 minutes [Fig.5e]. The Peltier plate below the gel enables to significantly accelerate the cooling. It is powered at 2.5A and enables to remove about 8 W from the top to the bottom. The Peltier is very efficient to cool down the system. The tip climbs back to the initial position in only 35 s [Fig.5.e]. Nevertheless, powering the Peltier plate requires 12 W which is dissipated into heat. It drives to a temperature increase of all the system (heat build-up). The heat sink placed underneath helps to cool the system.

In order to observe the active force exerted by the Braille tip during cooling, we conducted cyclic force test. Our force sensor is maintained at a fixed position over the tip. We then apply heating/cooling cycle while the tip is maintained at the low position and we measure the force in isostatic condition. The system is able to produce a force of 0.9 g over 10 cycles [Fig.5h]. The heating-cooling program is adjusted so that no heat build-up occurred even after all cycles.

If we dip the same HP-OR gel sample in a hot water bath, its height will quickly decrease from 5 mm to 2.9 mm. Therefore, we would expect a tip displacement of 2.1 mm which is 30% larger than the 1.4 mm actually measured.

To understand the discrepancy between the two experiments, we simulate the temperature through the entire Braille unit at equilibrium using the COMSOL software [Fig.6.a-b]. In the simulation model, the heat is injected homogeneously from the nichrome which is considered as a uniform 0.13 mm layer. The heat dissipation only happens through the bottom plate which is maintained at room temperature (20°C). Heat transport through the entire system only happens through diffusion considering the heat diffusion coefficient of each specific material. The convection in the water part is neglected.

The temperature trough the gel is not homogeneous [Fig.6a-b]. It is maximum at the top of the gel and minimum at the bottom [Fig.6.b] which is in contact with the plate where dissipation happens. Only a fraction of the gel has a temperature above the transition temperature (34°C). Therefore, only a fraction of the gel is going to shrink. For instance, at a heating power of 12%, only the top 75% of the gel is above $34\,°C$ and will shrink. Therefore, we expect the displacement to be only $2.1\,\text{mm} \times 75\,\% = 1.6\,\text{mm}$.

The tip displacement can be modeled for various heating power. At higher heating power, the maximum temperature increases and the gel fraction with a temperature above the transition temperature also increases. The tip displacement increases as a result. This prediction is actually confirmed with experiment. And we observe a good agreement between the model and the experimental observation [Fig.6c]. Despite its simplicity, our model shows that the temperature homogeneity is a limit to our system which reduces the actuation amplitude.

Finally, the single pin tip is tested under constant force to simulate the situation where a finger is kept on the pin tip throughout the actuation process [Fig5.d,f-g]. In the cold state, when we press on the tip it goes down because of the gel softness. Nevertheless, we still observe a relatively important actuation amplitude. It is observed that when a certain force is applied the gel at the swollen state it pinched a bit [Fig.5]. On the other hand, at the shrunk state gel was stiff enough to hold the tip at its place.

This experiment with constant force applied to the pin tip simulated the situation in which a fin-
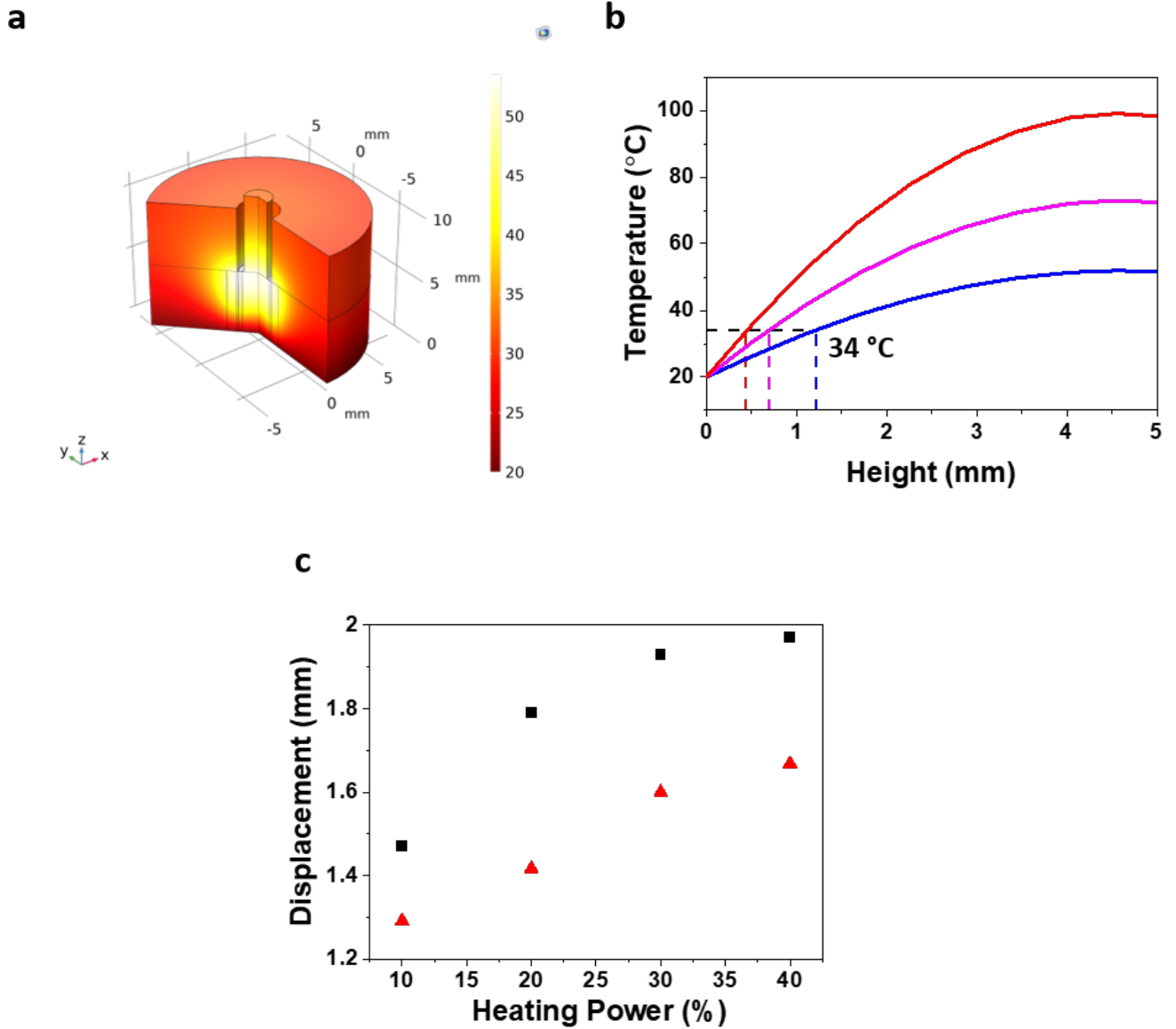
a

b

c

Figure 6: (a-b) 3D temperature distribution for the single pin Braille device obtained from COMSOL simulation operated at 12% heating power. (b) Temperature in the gel center along the vertical axis center at various heating power: (blue) 12%, (purple) 20% and (red) 30% power. Only a fraction of the gel is above the transition temperature (34 °C) and shrink. (c) Variation of the tip displacement amplitude for different heating power: (Red Triangle) experimental measurement and (Black Square) theoretical prediction based on COMSOL simulations.

ger would be held on top of the pin throughout the actuation process. When 2.5 g and 5.0g of force is applied to the tip, 0.75 mm and 0.66 mm displacement upon actuation was achieved. On the other hand, 75% and 60% of total displacement achieved during heating is recovered after 10 minutes of natural cooling, respectively [Fig.5.d]. These results show that even under 5.0 g of constant force on the Braille tip, more than 0.5 mm of displacement is reversibly preserved.

Then, the same pin tip displacement measure-ments are done by utilizing the Peltier for cooling. Under 2.5 g of force, the Braille pin tip descended for 0.8 mm upon heating but recovered 44% (0.35 mm) of the total displacement upon force cooling for 30s. Similarly, when 5.0 g was applied the pin tip descended for 0.5 mm recovering only 8% (0.04 mm) [Fig.5f].

From these results we can conclude that the same tip displacement cannot be achieved under differ-ent stress conditions but the gel can still operate with considerable displacement values. According

to the literature, these values are more than enough for a visually impaired individual to be able to sense the height difference of the pins during operation.[6]

3 Discussion

In this article, we present a fast actuating macroporous PNIPAM gel (MP gel) suitable for smart tactile display applications. PNIPAM holds high potential as a soft actuator since temperature is an easily controlled and adjusted stimuli. This makes the thermo-responsive gel very practical in fast actuation applications. The rate limiting factor in shrinking/re-swelling response of such gel is determined to be the diffusion of water through the gel. Thus, we synthesized gel with macroporosity to facilitate the water transport.

For "classical" organically reticulated gel (OR gel), the addition of macroporosity highly improve both the shrinking and re-swelling speed. It goes from hours for bulk gel to less than a minute for MP gel. OR gel with high porosity (HP-OR gel) shows a particularly adapted reaction time: the shrinking and re-swelling durations are respectively 15 s and 20 s.

Nevertheless we observe that re-swelling is systematically slower than shrinking. This asymmetry—also observed for bulk gel—is not yet fully understood. It is probably due to hysteresis of the pores structure during the gel collapse. But further studies would be required to understand it and eventually prevent it.

We also considered nanocomposite gel (NC gel) produced by the addition of clay nanoparticles. NC gel was very promising as bulk NC gel present both improved mechanical properties and a relatively fast shrinking kinetics. Nevertheless, macroporous NC gel happens to be unadapted for actuation. Indeed, macroporosity help to accelerate the shrinking but does not modify the re-swelling speed. re-swelling of both bulk and macroporous NC gel is particularly slow. And it appears that the water diffusion is not the limiting kinetics factor for NC gel re-swelling.

The cyclic compressive tests on HP-OR gels also proved a very good preservation of the initial elastic modulus even after 100 cycles. Creation of macroporosity into the gel highly improves its robustness as observed previously for other gel.[53] Whereas most materials are more fragile when porosity is added.

A cost-efficient smart single pin Braille system is designed and fabricated. Swift and precise temperature control over the gel volume is proved to be easily applicable. An optimum heating procedure where the temperature of the system can be swiftly controlled. With such method, a maximum recoverable pin tip displacement of 1.4 mm is achieved.

Using numerical simulation (on COMSOL), we demonstrated that the temperature is not homogeneous. This inhomogeneity reduces the maximum displacement by 25 %. Indeed a portion of the gel is heated over the transition temperature. A better design of the heating system will enable to access to the full potential of our system. .

The forced cooling system (Peltier) accelerated the pin tip ascension still preserving the 1.4 mm displacement amplitude. However, the cyclic repeatability of the same amplitude deteriorated due to the heat build-up in the system. This problem could be preventing by using a smaller Peltier plate and improving the cooling procedure. This way the cooling performance of the Peltier can be preserved over many heating-cooling cycles.

4 Conclusion

In this study, a fast actuating PNIPAM hydrogel is developed. The actuation speed is enhanced towards the requirements of a Braille device. To do so, we accelerated the solvent diffusion by the introduction of macroporosity through the gel. We characterized the impact of two distinct pore geometries and densities. We demonstrated that measuring the re-swelling dynamic is critical as swelling is much slower than shrinking. This difference of dynamic is also observed in the literature but is poorly understood. Comprehension of this asymmetry would be a key for a future work. Nevertheless, producing gel with a very high porosity enables to strongly reduce this asymetry. Hence, HP-OR gel show a quick dynamic of both shrinking and re-swelling. Additionally, we tested nanocomposite gel which show enhanced mechanical robustness. Unfortunately, we demonstrate this physically crosslinked gel did not perform optimally and is not adapted for actuation. It shows a very slow re-swelling dynamic which cannot be improved by adding porosity.

Effect of macroporosity on the mechanical properties have also been investigated. Adding porosity decreases the gel elastic modulus and therefore the potential force produced by the gel when

swelling. Especially, HP-OR gel show a more important modulus decrease than expected. It is probably due to an inadapted process to generate macroporosity. Macroporous PNIPAM gel offer a high potential for future improvement .

HP-OR gel show good enough properties for actuation. Therefore, we have developed a cost efficient Braille device. We demonstrate that our device enable to quickly tune the temperature of a water reservoir. A MP gel sample –placed in the center of the reservoir– can efficiently lift a pin. We demonstrate the cyclic performance and the high potential of our novel actuator for future smart Braille devices. We also provide a precise analysis of the temperature distribution. It will help to improve the design of our device and to increase the heating efficiency. Especially, the development of a Braille system with an arrays of pins (8 pins for a single array) is planned for a future work. This way we will be able to display letters and even images.

5 Materials and Methods

5.1 Bulk Gel and MP Gel Synthesis

N-isopropylacrylamide monomer (NIPAM), N, N'-methylenebis (acrylamide) (MBIS), ammonium persulfate (APS), N,N,N',N'-tetramethylethylenediamine (TEMED) and 2,2-Di-methoxy-2-phenylacetophenone (Irgacure 651) were purchased from Sigma-Aldrich. Lapo-nite RDS was received from BYK-Chemie GmbH. Colacryl DP300 and D150 (PMMA) were supplied generously from Lucite International Specialty Polymers and Resins Ltd. Shellac flakes were purchased from Dieter Schmid Werkzeuge GmbH. All chemicals are used as received without further purification.

Preparation of bulk nanocomposite gel (NC) is as follows. NIPAM monomer (2.26 g, 1.3 M) is dissolved in 15 ml pure water. After fully dissolving the monomer, Laponite-RDS (1.52 g, 7.7 wt.%) is slowly added to the solution under high speed stirring to prevent coagulation during mixing. The solution takes a homogeneous semi-transparent cloudy appearance upon laponite addition. After addition of the initiator APS, the solution is put into an ice-bath and purged with nitrogen for 15 minutes. Finally, the solution is poured into the cylindrical 2x4 mm and 4x4 mm (DIxH) molds after addition of 16 µl of TEMED. Polymerization took place at room temperature for 20 hours.

Preparation of organic reticulated gel (OR) is as followed. NIPAM monomer (2.26g – 1.2 M) is dissolved in 17.1 ml of pure water. Then, 1.9 ml of a solution MBIS in water (3wt%) and 100 µl of a solution of Irgacure 651 in ethanol (10wt%) are added. Solution is poured into the mold and placed under the UV lamp inside an ice-bath for 5min.

The OR solution for porous samples was prepared as follows. 2.26 g of NIPAM (1.2M) was dissolved in 17.1 ml of pure water. 1.9 ml of 3 wt.% aqueous MBIS solution is added. A 10 wt.% Irgacure solution in ethanol was prepared in an Eppendorf and 100 µl was added to the main mixture instead of APS and TEMED.

HP-OR gel. The template is made from PMMA micro-particles.[53] The particles are poured in a cylindrical glass mold (DxH: 7x10 mm for compression and shrinking/re-swelling tests and 4x4 mm for the single pin braille setup) and packed by applying a gentle pressure. Particles are sintered at 185°C for 8h to acquire PMMA scaffolds. These scaffolds are soaked into the monomer solution under vacuum for 4h and then left over-night to allow full absorption of the solution inside the scaffolds. The scaffolds were then taken out of the solutions and placed under the UV lamp inside an ice-bath for 20 minutes each side. The polymerized samples are rinsed with ethyl acetate for 4 days by refreshing the solutions every 24h. The HP-OR gels are then rinsed in ethanol and swollen in pure water before further utilization.

LP-NC and LP-OR gel. The shellac microfibers are produced by using a cotton candy machine (VEVOR-FR). The shellac flakes are melted at 170°C (125 V) and collected by an aluminum rod coated with a paper towel. In order to remove any hydrophobic contaminants, the fibers are rinsed with excess ultrapure water and dried at room temperature for 3 days. The shellac floss which is tightly packed during drying are placed in a petri dish. For LP-NC gel, the monomer solution is injected in between the floss and left to polymerize at room temperature for 20 hours. For the LP-OR gel, the petri dish is placed under UV and inside an ice bath for 20 minutes. Cylindrical samples with 2mm and 4 mm diameters were cut out from the polymerized OR and NC gel by using hole-punch and placed in a 0.5 M NaOH solution to leach the shellac fibers out of the gel matrix. The gels are left in NaOH solution under constant agitation by changing the solution every 24h until shellac fibers are visibly removed. Then, the gels

are washed in water bath.

5.2   Shrinking/Re-Swelling Test

All the gel samples were swollen in cold (20°C) pure water prior to any tests. Short time responses (minutes) is measured as followed. For the shrinking kinetic, we quickly dipped the cold gel in a hot water bath at 60°C. To measure the swelling kinetic, we take a shrunk gel sample (initialy soaked at 60°c for 5 min) and transfer it quickly to a bath at room temperature (20°C). The evolution of the gel sample is recorded by a camera (Thorlab). The resulting images are analyzed with ImageJ program. We extract the observed surface of the gel. We deduce the variation of volume by assuming the size variation is isotropic. The volume V is then given by $V/V_0 = (S/S_0)^{(3/2)}$ where V_0 and S_0 are respectively the initial volume and initial observed surface area.

Long time response (hours to days) is measured by dipping the gel in a hot water bath. We weighted the gel regularly to measure the volume evolution. Between each weighing, the gel is kept in water in a 60°C oven to keep the temperature constant.

5.3   Mechanical Test

In order to characterize the swollen gels mechanically, compression tests are performed. A mechanical testing machine (Mark-10 ESM301) is used. Both Young's modulus and compression strength at certain strain values are determined for all samples. To determine the true stress and the Young's modulus values, we assume to have a Poisson ratio of 0.5 (in-compressible material). The Young's modulus values are determined in the range of 10-20 % deformation for all samples.

5.4   3D Printing

The designs for the printing were produced using FreeCAD (version-0.19) software. The containment systems for the thermo-sensitive gels were produced by stereo-lithography method using DWS 29J+ 3-D printer. DS-3000 was used as the resin for the main body of the containment unit and the tactile surface whereas DL260 was used for the pin.

5.5   Tip Displacement Test

For the braille pin displacement measurements, Dual Mode Muscle Lever (300C, Aurora Scientific) is used. It allows to precisely measure the displacement of the pin while applying a controlled force. We typically applied a force of 0 mN, 25 mN (2.5g) or 50 mN (5g) in order to better simulate stress condition of human touch.

5.6   Comsol Simulation

The COMSOL simulation is constructed in 2D-axisymmetric space with using heat transfer in solids in a stationary mode. Since 2D-axisymmetry is utilized one half of the 2D system is constructed. A gel containment unit with 1.185x5 mm (WxH), nichrome layer with 0.13x5 mm (WxH), stainless steel layer between the gel containment unit and nichrome layer with 0.25x5 mm (WxH) dimensions are constructed. A water consisting layer surrounding the nichrome layer with 0.25x5 mm (WxH) is also added. The outer layer of the system consisted of 5.5x5 mm (WxH) acrylic shell. The pin also designed from acrylic with dimensions of 1x6 mm (WxH). The acrylic cap had the dimensions of 6.25x5 mm (WxH).The simulation is done in stationary mode without any time dependency. Only conduction is used for the heat transfer by considering heat diffusion coefficient for each part where the convection in the water phase is neglected.

5.7   Cyclic Braille Tip Force Test

For measuring the force exerted by the Braille tip during cooling of the gel, the single pin Braille setup is placed on the lower head of the MARK-10 instrument. The system is heated to acquire full retraction of the pin tip force applied. This position is fixed throughout the experiment.The system is cooled naturally until the exerted force on the upper head is fixed. Force heating with full power for 2s and with 12% power for 3 minutes is applied.Afterwards force cooling with full power for 2 seconds and natural cooling for 15 minutes is exerted.These heating/cooling programs were applied periodically for 10 successive cycles.

Supporting Information Available

Data on mass change experiments of the gels samples upon heating and cooling, cyclic compression test results of the remaining samples, images of the sacrificial scaffolds;PDF.

References

(1) Yang, W.; Huang, J.; Wang, R.; Zhang, W.; Liu, H.; Xiao, J. A Survey on Tactile Displays for Visually Impaired People. *IEEE Transactions on Haptics* **2021**, *14*, 712–721.

(2) Grigorii, R. V.; Colgate, J. E.; Klatzky, R. The spatial Profile of Skin Indentation Shapes Tactile Perception Across Stimulus Frequencies. *Scientific Reports* **2022**, *12*, 1–11.

(3) Kim, J.; Han, B. K.; Pyo, D.; Ryu, S.; Kim, H.; Kwon, D. S. Braille Display for Portable Device Using Flip-Latch Structured Electromagnetic Actuator. *IEEE Transactions on Haptics* **2020**, *13*, 59–65.

(4) Leonardis, D.; Loconsole, C.; Frisoli, A. A Passive and Scalable Magnetic Mechanism for Braille Cursor, an Innovative Refreshable Braille Display. *Meccanica* **2020**, *55*, 1639–1653.

(5) Smithmaitrie, P.; Kanjantoe, J.; Tandayya, P. Touching Force Response of the Piezoelectric Braille Cell. *i-CREATe 2007 - Proceedings of the 1st International Convention on Rehabilitation Engineering and Assistive Technology in Conjunction with 1st Tan Tock Seng Hospital Neurorehabilitation Meeting* **2007**, 174–178.

(6) Runyan, N. H.; Carpi, F. Seeking the 'Holy Braille' Display: Might Electromechanically Active Polymers Be the Solution? *Expert Review of Medical Devices* **2011**, *8*, 529–532.

(7) Tian, X.; Sun, Y.; Li, Z.; Wang, H.; Wang, Z.; Wang, H.; Zhu, J.; Yang, Z. Design and Experiment Using Flexible Bumps for Piezoelectric-Driven Hydraulically Amplified Braille Dot Display. *Micromachines* **2021**, *12*.

(8) Velázquez, R.; Hernández, H.; Preza, E. A Portable Piezoelectric Tactile Terminal for Braille Readers. *Applied Bionics and Biomechanics* **2012**, *9*, 45–60.

(9) Prescher, D.; Bornschein, J.; Köhlmann, W.; Weber, G. Touching Graphical Applications: Bi-manual Tactile Interaction on the Hyper-Braille Pin-Matrix Display. *Universal Access in the Information Society* **2018**, *17*, 391–409.

(10) Russomanno, A.; Xu, Z.; O'Modhrain, S.; Gillespie, B. A Pneu Shape Display: Physical Buttons with Programmable Touch Response. *2017 IEEE World Haptics Conference, WHC 2017* **2017**, 641–646.

(11) Qiu, Y.; Lu, Z.; Pei, Q. Refreshable Tactile Display Based on a Bistable Electroactive Polymer and a Stretchable Serpentine Joule Heating Electrode. *ACS Applied Materials and Interfaces* **2018**, *10*, 24807–24815.

(12) Bowles, A.; Rahman, A.; Jarman, T.; Morris, P.; Gore, J. A New Technology for High Density Actuator Arrays. *Smart Structures and Materials 2005: Smart Structures and Integrated Systems* **2005**, *5764*, 680.

(13) Zárate, J. J.; Shea, H. Using Pot-Magnets to Enable Stable and Scalable Electromagnetic Tactile Displays. *IEEE Transactions on Haptics* **2017**, *10*, 106–112.

(14) Cestarollo, L.; Smolenski, S.; El-Ghazaly, A. Nanoparticle-Based Magnetorheological Elastomers with Enhanced Mechanical Deflection for Haptic Displays. *ACS Applied Materials and Interfaces* **2022**, *14*, 19002–19011.

(15) Velázquez, R.; Pissaloux, E. E.; Hafez, M.; Szewczyk, J. Tactile Rendering with Shape-Memory-Alloy Pin-Matrix. **2008**, *57*, 1051–1057.

(16) Matsunaga, T.; Totsu, K.; Esashi, M.; Haga, Y. Tactile Display Using Shape Memory Alloy Micro-Coil Actuator and Magnetic Latch Mechanism. *Displays* **2013**, *34*, 89–94.

(17) Frediani, G.; Busfield, J.; Carpi, F. Enabling Portable Multiple-Line Refreshable Braille Displays With Electroactive Elastomers. *Medical Engineering and Physics* **2018**, *60*, 86–93.

(18) Feng, G. H.; Hou, S. Y. Investigation of Tactile Bump Array Actuated with Ionic Polymer–Metal Composite Cantilever Beams for Refreshable Braille Display Application. *Sensors and Actuators, A: Physical* **2018**, *275*, 137–147.

(19) Ankit,; Tiwari, N.; Rajput, M.; Chien, N. A.; Mathews, N. Highly Transparent and Integrable Surface Texture Change Device for Localized Tactile Feedback. *Small* **2018**, *14*, 1–9.

(20) Gil, E. S.; Hudson, S. M. Stimuli-Responsive Polymers and Their Bioconjugates. *Progress in Polymer Science (Oxford)* **2004**, *29*, 1173–1222.

(21) Ahn, S. K.; Kasi, R. M.; Kim, S. C.; Sharma, N.; Zhou, Y. Stimuli-Responsive Polymer Gels. *Soft Matter* **2008**, *4*, 1151–1157.

(22) Ionov, L. Polymeric actuators. *Langmuir* **2015**, *31*, 5015–5024.

(23) Haq, M. A.; Su, Y.; Wang, D. Mechanical Properties of PNIPAM Based Hydrogels: A Review. *Materials Science and Engineering C* **2017**, *70*, 842–855.

(24) Liu, J.; Jiang, L.; He, S.; Zhang, J.; Shao, W. Recent Progress in PNIPAM-Based Multi-Responsive Actuators: A Mini-Review. *Chemical Engineering Journal* **2022**, *433*, 133496.

(25) Depa, K.; Strachota, A.; Šlouf, M.; Hromádková, J. Fast Temperature-Responsive Nanocomposite PNIPAM Hydrogels with Controlled Pore Wall Thickness: Force and Rate of T-Response. *European Polymer Journal* **2012**, *48*, 1997–2007.

(26) Hosseini, H.; Tenhu, H.; Hietala, S. Rheological Properties of Thermoresponsive Nanocomposite Hydrogels. *Journal of Applied Polymer Science* **2016**, *133*, 2–7.

(27) Kim, S.; Lee, K.; Cha, C. Refined Control of Thermoresponsive Swelling/Deswelling and Drug Release Properties of Poly(N-isopropylacrylamide) Hydrogels Using Hydrophilic Polymer Crosslinkers. *Journal*

(28) Belali, S.; Savoie, H.; O'Brien, J. M.; Cafolla, A. A.; O'Connell, B.; Karimi, A. R.; Boyle, R. W.; Senge, M. O. Synthesis and Characterization of Temperature-Sensitive and Chemically Cross-Linked Poly(N-isopropylacrylamide)/Photosensitizer Hydrogels for Applications in Photodynamic Therapy. *Biomacromolecules* **2018**, *19*, 1592–1601.

(29) Li, J.; Mooney, D. J. Designing Hdrogels for Controlled Drug Delivery. *Nature Reviews Materials* **2016**, *1*, 1–18.

(30) Chen, Y.; Liu, W.; Zeng, G.; Liu, Y. J. Microporous PDMAEMA-Based Stimuli-Responsive Hydrogel and Its Application in Drug Release. *Journal of Applied Polymer Science* **2017**, *134*, 1–12.

(31) Anaraki, V.; Abtahi, S. M. M.; Farhood, B.; Ejtemai-fard, M. A Novel Method for Increasing the Sensitivity of NIPAM Polymer Gel Dosimeter. *Radiation Physics and Chemistry* **2018**, *153*, 35–43.

(32) Senden, R. J.; De Jean, P.; McAuley, K. B.; Schreiner, L. J. Polymer Gel Dosimeters with Reduced Toxicity: A Preliminary Investigation of the NMR and Optical Dose-Response Using Different Monomers. *Physics in Medicine and Biology* **2006**, *51*, 3301–3314.

(33) Inal, S.; Kölsch, J. D.; Sellrie, F.; Schenk, J. A.; Wischerhoff, E.; Laschewsky, A.; Neher, D. A Water Soluble Fluorescent Polymer as a Dual Colour Sensor for Temperature and a Specific Protein. *Journal of Materials Chemistry B* **2013**, *1*, 6373–6381.

(34) Hu, X.; Ge, Z.; Wang, X.; Jiao, N.; Tung, S.; Liu, L. Multifunctional Thermo-Magnetically Actuated Hybrid Soft Millirobot Based on 4D Printing. *Composites Part B: Engineering* **2022**, *228*, 109451.

(35) Breger, J. C.; Yoon, C.; Xiao, R.; Kwag, H. R.; Wang, M. O.; Fisher, J. P.; Nguyen, T. D.; Gracias, D. H. Self-Folding

Thermo-Magnetically Responsive Soft Microgrippers. *ACS Applied Materials and Interfaces* **2015**, *7*, 3398–3405.

(36) Gong, J. P.; Katsuyama, Y.; Kurokawa, T.; Osada, Y. Double-Network Hydrogels with Extremely High Mechanical Strength. *Advanced Materials* **2003**, *15*, 1155–1158.

(37) Zheng, W. J.; An, N.; Yang, J. H.; Zhou, J.; Chen, Y. M. Tough Al-Alginate/Poly(N - isopropylacrylamide) Hydrogel with Tunable LCST for Soft Robotics. *ACS Applied Materials and Interfaces* **2015**, *7*, 1758–1764.

(38) Chen, Q.; Chen, H.; Zhu, L.; Zheng, J. Fundamentals of Double Network Hydrogels. *Journal of Materials Chemistry B* **2015**, *3*, 3654–3676.

(39) Gil, E. S.; Hudson, S. M. Effect of Silk Fibroin Interpenetrating Networks on Swelling/Deswelling Kinetics and Rheological Properties of Poly(N-isopropylacrylamide) Hydrogels. *Biomacromolecules* **2007**, *8*, 258–264.

(40) Wang, J.; Lin, L.; Cheng, Q.; Jiang, L. A Strong Bio-Inspired Layered PNIPAM-Clay Nanocomposite Hydrogel. *Angewandte Chemie - International Edition* **2012**, *51*, 4676–4680.

(41) Warren, H.; Shepherd, D. J.; in het Panhuis, M.; Officer, D. L.; Spinks, G. M. Porous PNIPAm Hydrogels: Overcoming Diffusion-Governed Hydrogel Actuation. *Sensors and Actuators, A: Physical* **2020**, *301*, 111784.

(42) Haraguchi, K.; Li, H. J. Mechanical Properties and Structure of Polymer-Clay Nanocomposite Gels with High Clay Content. *Macromolecules* **2006**, *39*, 1898–1905.

(43) Haraguchi, K.; Li, H. J.; Song, L.; Murata, K. Tunable optical and swelling/deswelling properties associated with control of the coil-to-globule transition of poly(N-isopropylacrylamide) in polymer - Clay nanocomposite gels. *Macromolecules* **2007**, *40*, 6973–6980.

(44) Haraguchi, K.; Song, L. Microstructures Formed in Co-Cross-Linked Networks and Their Relationships to the Optical and Mechanical Properties of PNIPA/Clay Nanocomposite Gels. *Macromolecules* **2007**, *40*, 5526–5536.

(45) Depa, K.; Strachota, A.; Šlouf, M.; Brus, J. Poly(N-isopropylacrylamide)-SiO2 Nanocomposites Interpenetrated by Starch: Stimuli-Responsive Hydrogels with Attractive Tensile Properties. *European Polymer Journal* **2017**, *88*, 349–372.

(46) Xia, X.; Yih, J.; D'Souza, N. A.; Hu, Z. Swelling and Mechanical Behavior of Poly (N-isopropylacrylamide)/Na-montmorillonite Layered Silicates Composite Gels. *Polymer* **2003**, *44*, 3389–3393.

(47) Strachota, B.; Hodan, J.; Matějka, L. Poly(N-isopropylacrylamide)-Clay Hydrogels: Control of Mechanical Properties and Structure by the Initiating Conditions of Polymerization. *European Polymer Journal* **2016**, *77*, 1–15.

(48) Haraguchi, K.; Takehisa, T.; Fan, S. Effects of Clay Content on the Properties of Nanocomposite Hydrogels Composed of poly(N-isopropylacrylamide) and Clay. *Macromolecules* **2002**, *35*, 10162–10171.

(49) Haraguchi, K. Nanocomposite Hydrogels. *Current Opinion in Solid State and Materials Science* **2007**, *11*, 47–54.

(50) Quesada-Pérez, M.; Maroto-Centeno, J. A.; Forcada, J.; Hidalgo-Alvarez, R. Gel Swelling Theories: The Classical Formalism and Recent Approaches. *Soft Matter* **2011**, *7*, 10536–10547.

(51) Yoon, J.; Cai, S.; Suo, Z.; Hayward, R. C. Poroelastic Swelling Kinetics of Thin Hydrogel Layers: Comparison of Theory and Experiment. *Soft Matter* **2010**, *6*, 6004.

(52) Huerta-Angeles, G.; Hishchak, K.; Strachota, A.; Strachota, B.; Šlouf, M.; Matějka, L. Super-Porous Nanocomposite PNIPAm Hydrogels Reinforced with Titania Nanoparticles, Displaying a Very Fast Temperature Response as Well as pH-Sensitivity. *European Polymer Journal* **2014**, *59*, 341–352.

(53) Mansard, V. A Macroporous Smart Gel Based on a pH-Sensitive Polyacrylic Polymer for the Development of Large Size Artificial Muscles with Linear Contraction. *Soft Matter* **2021**, *17*, 9644–9652.

(54) Zhao, Q.; Sun, J.; Ling, Q.; Zhou, Q. Synthesis of Macroporous Thermosensitive Hydrogels: A Novel Method of Controlling Pore Size. *Langmuir* **2009**, *25*, 3249–3254.

(55) Ziółkowski, B.; Florea, L.; Theobald, J.; Benito-Lopez, F.; Diamond, D. Porous Self-Protonating Spiropyran-Based NIPAAm Gels with Improved Reswelling Kinetics. *Journal of Materials Science* **2016**, *51*, 1392–1399.

(56) Alsaid, Y.; Wu, S.; Wu, D.; Du, Y.; Shi, L.; Khodambashi, R.; Rico, R.; Hua, M.; Yan, Y.; Zhao, Y.; Aukes, D.; He, X. Tunable Sponge-Like Hierarchically Porous Hydrogels with Simultaneously Enhanced Diffusivity and Mechanical Properties. *Advanced Materials* **2021**, *33*, 1–9.

(57) Hua, M.; Wu, S.; Ma, Y.; Zhao, Y.; Chen, Z.; Frenkel, I.; Strzalka, J.; Zhou, H.; Zhu, X.; He, X. Strong Tough Hydrogels via the Synergy of Freeze-Casting and Salting Out. *Nature* **2021**, *590*, 594–599.

(58) Gil, E. S.; Park, S. H.; Tien, L. W.; Trimmer, B.; Hudson, S. M.; Kaplan, D. L. Mechanically Robust, Rapidly Actuating, and Biologically Functionalized Macroporous Poly(N-isopropylacrylamide)/Silk Hybrid Hydrogels. *Langmuir* **2010**, *26*, 15614–15624.

(59) Deng, Z.; Yu, R.; Guo, B. Stimuli-Responsive Conductive Hydrogels: Design, Properties and Applications. *Materials Chemistry Frontiers* **2021**, *5*, 2092–2123.

TOC Graphic

Porous PNIPAM Gel

PNIPAM   Single Pin Braille Device